

Resonance-Activated Spin-Flipping for Efficient Organic Ultralong Room-Temperature Phosphorescence

Ye Tao, Runfeng Chen,* Huanhuan Li, Jie Yuan, Yifang Wan, He Jiang, Cailin Chen, Yubing Si, Chao Zheng, Baocheng Yang, Guichuan Xing, and Wei Huang*

Triplet-excited-state-involved photonic and electronic properties have attracted tremendous attention for next-generation technologies. To populate triplet states, facile intersystem crossing (ISC) for efficient exciton spin-flipping is crucial, but it remains challenging in organic molecules free of heavy atoms. Here, a new strategy is proposed to enhance the ISC of purely organic optoelectronic molecules using heteroatom-mediated resonance structures capable of promoting spin-flipping at large singlet–triplet splitting energies with the aid of the fluctuation of the state energy and n-orbital component upon self-adaptive resonance variation. Combined experimental and theoretical investigations confirm the key contributions of the resonance variation to the profoundly promoted spin-flipping with ISC rate up to $\approx 10^7 \text{ s}^{-1}$ in the rationally designed $\text{N}=\text{P}=\text{X}$ ($\text{X} = \text{O}$ or S) resonance molecules. Importantly, efficient organic ultralong room-temperature phosphorescence (OURTP) with simultaneously elongated lifetime and improved efficiency results overcoming the intrinsic competition between the OURTP lifetime and efficiency. With the spectacular resonance-activated OURTP molecules, time-resolved and color-coded quick response code devices with multiple information encryptions are realized, demonstrating the fundamental significance of this approach in boosting ISC dynamically for advanced optoelectronic applications.

Organic ultralong room-temperature phosphorescence (OURTP), which has a very long emission lifetime over 100 ms at ambient conditions, brings unique material characteristics of purely organic luminogens recently for state-of-the-art optoelectronic device applications that cannot be realized using conventional fluorescent and phosphorescent molecules.^[1–9]

A large variety of optoelectronic and bio-scientific applications including organic light-emitting diodes (OLEDs),^[10] anti-counterfeiting,^[11,12] optical recording,^[13] sensors,^[14] and bioimaging^[15,16] can be updated based on the extraordinary photophysical processes of OURTP emission that occur via the triplet excited states. However, OURTP still suffers the low emission efficiency and a small range of applicable materials owing to its phosphorescent nature that requires facile intersystem crossing (ISC) to transform the photoexcited singlet exciton to the triplet one via spin-flipping, which is spin forbidden and significantly difficult for common organic optoelectronic molecules without heavy atoms. It should also be noted that the ability to enhance ISC between the excited states of purely organic materials with different spin multiplicity is also of key importance in current organic electronics for the design of high-performance and new-functional organic optoelectronic molecules, including thermally activated delay fluorescence (TADF), triplet–triplet annihilation (TTA), and singlet fission (SF) materials, for advanced optoelectronic applications.^[17–20]

Two basic guidelines to promote exciton spin-flipping for facile ISC have been developed.^[21,22] The first one is the energy gap law, which requires matched energy levels of the two states with small singlet–triplet splitting (ΔE_{ST}) for a thermal

Two basic guidelines to promote exciton spin-flipping for facile ISC have been developed.^[21,22] The first one is the energy gap law, which requires matched energy levels of the two states with small singlet–triplet splitting (ΔE_{ST}) for a thermal

Dr. Y. Tao, Prof. R. F. Chen, Dr. H. H. Li, J. Yuan, Y. F. Wan, H. Jiang, C. L. Chen, Dr. C. Zheng, Prof. W. Huang
Key Laboratory for Organic Electronics and Information Displays
and Jiangsu Key Laboratory for Biosensors
Institute of Advanced Materials (IAM)
Jiangsu National Synergetic Innovation Center
for Advanced Materials (SICAM)
Nanjing University of Posts and Telecommunications
9 Wenyuan Road, Nanjing 210023, China
E-mail: iamrfchen@njupt.edu.cn; wei-huang@njtech.edu.cn

Dr. Y. Tao, Prof. G. C. Xing, Prof. W. Huang
Key Laboratory of Flexible Electronics (KLOFE) and Institute
of Advanced Materials (IAM)
Jiangsu National Synergetic Innovation Center for Advanced Materials
(SICAM)
Nanjing Tech University (Nanjing Tech)
30 South Puzhu Road, Nanjing 211816, China
Dr. Y. B. Si, Prof. B. C. Yang
Henan Provincial Key-Laboratory of Nano-Composite and Applications
Institute of Nanostructured Functional Materials
Huanghe Science and Technology College
Zhengzhou, Henan 450006, China

 The ORCID identification number(s) for the author(s) of this article can be found under <https://doi.org/10.1002/adma.201803856>.

DOI: 10.1002/adma.201803856

equilibrium of the singlet and triplet excited states.^[23] Typically illustrated in TADF emitters ($\Delta E_{ST} < 0.37$ eV), efficient ISC and reverse ISC processes with corresponding rate constants up to $\approx 10^6$ and $\approx 10^4$ s⁻¹ have been observed and proved to be the main reason for their high OLED performance.^[18] The other guide for enhancing exciton transformation is the El-Sayed rule,^[24,25] which suggests that the $^1(\pi, \pi^*) \rightarrow ^3(n, \pi^*)$ transition is faster than that of $^1(\pi, \pi^*) \rightarrow ^3(\pi, \pi^*)$ and $^1(n, \pi^*) \rightarrow ^3(\pi, \pi^*)$ is more facile than $^1(n, \pi^*) \rightarrow ^3(n, \pi^*)$. Consequently, the participation of heteroatom in the π -conjugated system is suggested to be mandatory to present n orbitals perpendicular to the π orbitals in triggering striking spin-orbital coupling (SOC) for ISC via either the nonpair electrons or the empty orbitals of the incorporated heteroatoms.

Resonance structures, previously proposed to describe delocalized electrons within certain molecules, were found to be effective in selectively and dynamically modulating the electronic properties of organic semiconductors by taking advantages of the facile resonance interconversion between different canonical forms for in situ response to the electronic environmental variations.^[26] The energy difference between the enantiotropic Lewis structures of the resonance adaptive molecules, defined as the activation energy of resonance variation (E_{RV}), is of fundamental paramount in tuning the self-adaptivity for balanced charge transport and high OLED performance.^[27] Resonance molecules with small E_{RV} show a much higher performance than that with large E_{RV} , when they are functioning as host materials of blue phosphorescent OLEDs.^[27] Nevertheless, from another point of view, large E_{RV} values between different canonical forms suggest that the molecular energies of resonance molecules are not constant but will fluctuate considerably in a large range when they respond to the external stimuli. Therefore, it can be expected that the varied excited state energies of the resonance molecules would significantly reduce the real-time ΔE_{ST} to promote ISC at a large static ΔE_{ST} , apparently in contradictory to but intrinsically in accordance with the energy-gap law (Figure 1a). Moreover, the resonance linkages are multi-heteroatom mediated, containing P, N, and O/S atoms in a π -conjugated aromatic architecture; efficient $n \rightarrow \pi^*$ transition with large changes of n -orbital participation manipulated by resonance variation is well supported to facilitate ISC, according to the El-Sayed rule (Figure 1b). Therefore, considering that both the energy-gap law and El-Sayed rule can be inherently fulfilled in the heteroatom-mediated resonance molecules, we can expect facile ISC processes for efficient spin-flipping upon resonance variation.

Here, in contrast to conventional methods in statically manipulating the excited states and ISC, we propose a dynamic approach to promote spin-flipping of purely organic optoelectronic molecules through heteroatom-mediated resonance structures. Indeed, resonance-enhanced ISC process with rate constant up to 9.7×10^6 s⁻¹, which is comparable to the highest ISC rate of recently reported TADF molecules,^[17] has been achieved in the N–P=S resonance molecule with a large ΔE_{ST} (>0.8 eV). Moreover, efficient OURTP emission with simultaneously elongated lifetime up to 0.67 s and improved quantum efficiency of 4.0% at ambient conditions was also resulted, breaking the intrinsic interference of OURTP lifetime and efficiency. Time-resolved and color-coded multiple

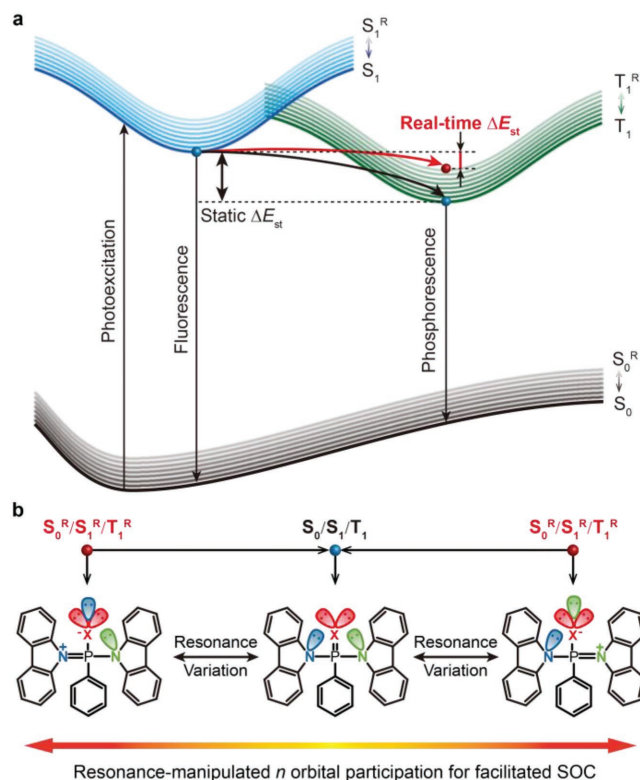


Figure 1. Schematic representation of resonance-activated spin-flipping for enhanced intersystem crossing. a) Resonance-enhanced ISC by reducing singlet–triplet splitting (ΔE_{ST}). Note that the lowest singlet (S_1) and triplet (T_1) excited states may vary in energy due to resonance variation for the corresponding S_1^R and T_1^R , resulting in reduced ΔE_{ST} in real time. b) Design of N–P=X (X = O and S) molecules with resonance-facilitated spin-orbital coupling (SOC) for OURTP emission. The n -orbital participation in resonance molecules could be effectively manipulated by resonance variation, resulting in high SOC to facilitate ISC.

informational quick response (QR) code application that can be read easily by commercial mobile phones is realized on flexible substrates, rendering the promising applications of these resonance OURTP materials in the field of information and data encryption.

To validate our hypothesis to promote spin-flipping for high ISC by resonance variation, we designed and synthesized two heteroatom-mediated resonance molecules of di(9*H*-carbazol-9-yl)(phenyl)phosphine oxide (DNCzPO) and di(9*H*-carbazol-9-yl)(phenyl)phosphine sulfide (DNCzPS) by incorporating organic luminophore of carbazole into resonance structures of N–P=O and N–P=S, respectively. Previously reported red OURTP molecule of di(9*H*-carbazol-9-yl)(phenyl)phosphine (DNCzP) was also prepared and investigated (Scheme S1, Supporting Information).^[2] DNCzPO and DNCzPS were conventionally synthesized through directly N–P coupling reaction followed by oxidation and sulfuration using hydrogen peroxide and sulfur, respectively. These two compounds are also excellent host materials of blue phosphorescent OLEDs.^[26,27] Detailed synthetic procedures and molecular structure characterizations are presented in the Supporting Information. Benefiting from the nonplanar configuration and stable resonance linkages,^[28] DNCzPO and DNCzPS have good solubility

in organic solvents and excellent thermal stabilities with high melting points (>220 °C) and decomposition temperature (>320 °C) (Figures S1 and S2, Supporting Information). Colorless single crystals and powders of **DNCzP**, **DNCzPO**, and **DNCzPS** can be obtained by slow evaporation of a mixed dichloromethane and ethanol solution at room temperature.

Except for the slightly blueshift absorption and emission spectra due to the effects of electron deficient $N^+=P-X^-$ canonical forms induced by the resonance variation, UV–vis absorption and fluorescence properties of the resonance molecules are very similar to that of **DNCzP** at room temperature (Figure S3, Supporting Information), showing $n \rightarrow \pi^*$ transition for absorption around 305 nm and two fluorescence bands around 342 and 355 nm in solution and around 410 and 430 nm in powder with short lifetimes about several nanoseconds (ns) (Figures S4–S7, Supporting Information).^[29] Excitingly, efficient OURTP emission can be observed when these molecules are in powder and are excited by UV light (365 nm) at room temperature (Figure 2a–c; Figure S8, Supporting Information). The OURTP color changes from the red of **DNCzP** to the greenish yellow of **DNCzPO** and the yellow of **DNCzPS** due to the shift and relative strength change of the afterglow emission bands (Figure 2a–c). Interestingly, OURTP performance of **DNCzPO** and **DNCzPS** powders is much higher than that of **DNCzP**; the OURTP quantum efficiency (Φ^{T^*}) increases from 0.08% of **DNCzP** to 2.8% of **DNCzPO** and 4.0% of **DNCzPS** and the OURTP lifetime (τ^{T^*}) elongates from 0.23 s of **DNCzP** to 0.51 s of **DNCzPS** and 0.67 s of **DNCzPO** (Table 1), clearly demonstrating the enhancements in both efficiency and lifetime of the resonance molecules. These lifetimes and efficiencies of OURTP emission are among the best results of OURTP materials.^[5,30,31] Moreover, in contrast to the conventional competition between the OURTP lifetime and efficiency,^[5] the heteroatom-mediated resonance molecules of **DNCzPO** and **DNCzPS** exhibit simultaneously high lifetime enlargement of ≈ 2 - and 3-folds and quantum efficiency enhancement of ≈ 35 - and 50-folds in OURTP emission than that of **DNCzP**, indicating the significant advantages of resonance structures in enhancing OURTP.

In a further set of experiments, the influences of atmosphere, UV-light intensity, excitation duration, and temperature on the extraordinary OURTP were investigated. The strength and lifetime of OURTP at 587 nm for **DNCzP**, 537 nm for **DNCzPO**, and 530 nm for **DNCzPS** are almost identical in different atmospheres of argon, air, and oxygen (Figures S9–S11, Supporting Information), suggesting that their OURTP is very stable and insensitive to varied atmospheres due to the effectively prevented quenching of the excited triplet excitons by blocking the penetration of oxygen molecules.^[12,14] When the UV-light excitation intensity increases, both the steady-state and OURTP luminescence strengthen significantly (Figure S12, Supporting Information). However, according to the excitation duration tests, the OURTP emission of the resonance molecules needs slightly more time (3–6 s) to reach constant intensity in comparison to that of **DNCzP** (≈ 2 s), probably due to the involvement of additional self-adaptive procedures to populate triplet excites via ISC (Figure S13, Supporting Information). The dynamic adaptation characteristics for self-adaptive tautomerization between multiple electronic states of

both neutral and charged resonance forms to promote spin-flipping by dynamically reducing ΔE_{ST} and enhancing lone-pair electron redistribution would require essentially additional time for OURTP emission.

To gain further information of the spectacular OURTP promoted by resonance variation, steady-state and time-resolved photoluminescence behaviors were investigated at low temperature (77 K). Owing to the suppressed nonradiative relaxation processes at 77 K,^[3] the phosphorescence is visible and its strength becomes comparable to or even higher than that of fluorescence in the steady-state PL spectra of the resonance molecules in dilute solution (Figure 2d). In solid powder state, the short-lived (≈ 10 ns) fluorescence redshifted to ≈ 420 nm and OURTP appears at ≈ 540 and ≈ 580 nm from the steady-state PL spectra at 77 K (Figure 2e). Time-resolved PL spectra with a 5 ms delay (Figure S14, Supporting Information) reveal that the phosphorescent peaks are located at 420–450 nm. Thus, three regions for the fluorescence (yellow), phosphorescence (green), and OURTP (red) of the resonance molecules at low temperature can be clarified. In general, when the temperature drops, both fluorescence and OURTP spectra are stable without apparent shifts but are refined and significantly enhanced with elongated lifetime and increased quantum efficiency, showing that the τ^{T^*} is up to 1.1 s and Φ^{T^*} are 2.8%, 5.7%, and 41.7% at 77 K for OURTP emission of **DNCzP**, **DNCzPO**, and **DNCzPS**, respectively (Table 1; Figures S5–S7 and S15–S17, Supporting Information).

With these elaborated photophysical data at both room temperature and 77 K, the rate constants of radiative and nonradiative relaxations of singlet and triplet excited states as well as ISC rate (k_{ISC}) can be figured out by establishing the corresponding photophysical kinetic equations based on the photoexcitation, exciton transformation, triplet trapping, and intermolecular phosphorescence for OURTP emission. Due to the spin-forbidden transition from the triplet excited state to the ground state, these molecules show very slow radiative ($k_r^{T^*}$) and nonradiative ($k_{nr}^{T^*}$) decay rates for the yellowish OURTP emission accompanied by the fast fluorescence decay (k_r^F) for strong blue prompt fluorescent emission.^[5,32] Interestingly, k_{ISC} of **DNCzPO** and **DNCzPS** powders reach 2.6×10^6 and 9.7×10^6 s⁻¹ at room temperature (Figure 2f), which are about 22- and 81-folds higher than that of **DNCzP** (1.2×10^5 s⁻¹), clearly suggesting the enhanced ISC with the aid of the heteroatom-mediated resonance variation. At low temperature (77 K), the nonradiative decay of both singlet and triplet excited states is significantly suppressed with much decreased decay rates and increased fluorescent and OURTP lifetimes and efficiencies. High k_{ISC} up to 8.9×10^7 s⁻¹, which is even higher than k_r^F (3.8×10^7 s⁻¹), has been observed in **DNCzPS** powder at 77 K (Table S1, Supporting Information). Again, the resonance molecules of **DNCzPO** and **DNCzPS** show much higher k_{ISC} than that of **DNCzP**. The significantly promoted spin-flipping of resonance molecules in solid state was also observed in dilute solution at 77 K (Table S2, Supporting Information), further suggesting the significant enhancement effects of the resonance variations on ISC.

To theoretically understand the exact reasons for the promoted ISC in resonance molecules, we performed first-principles time-dependent density functional theory (TD-DFT)

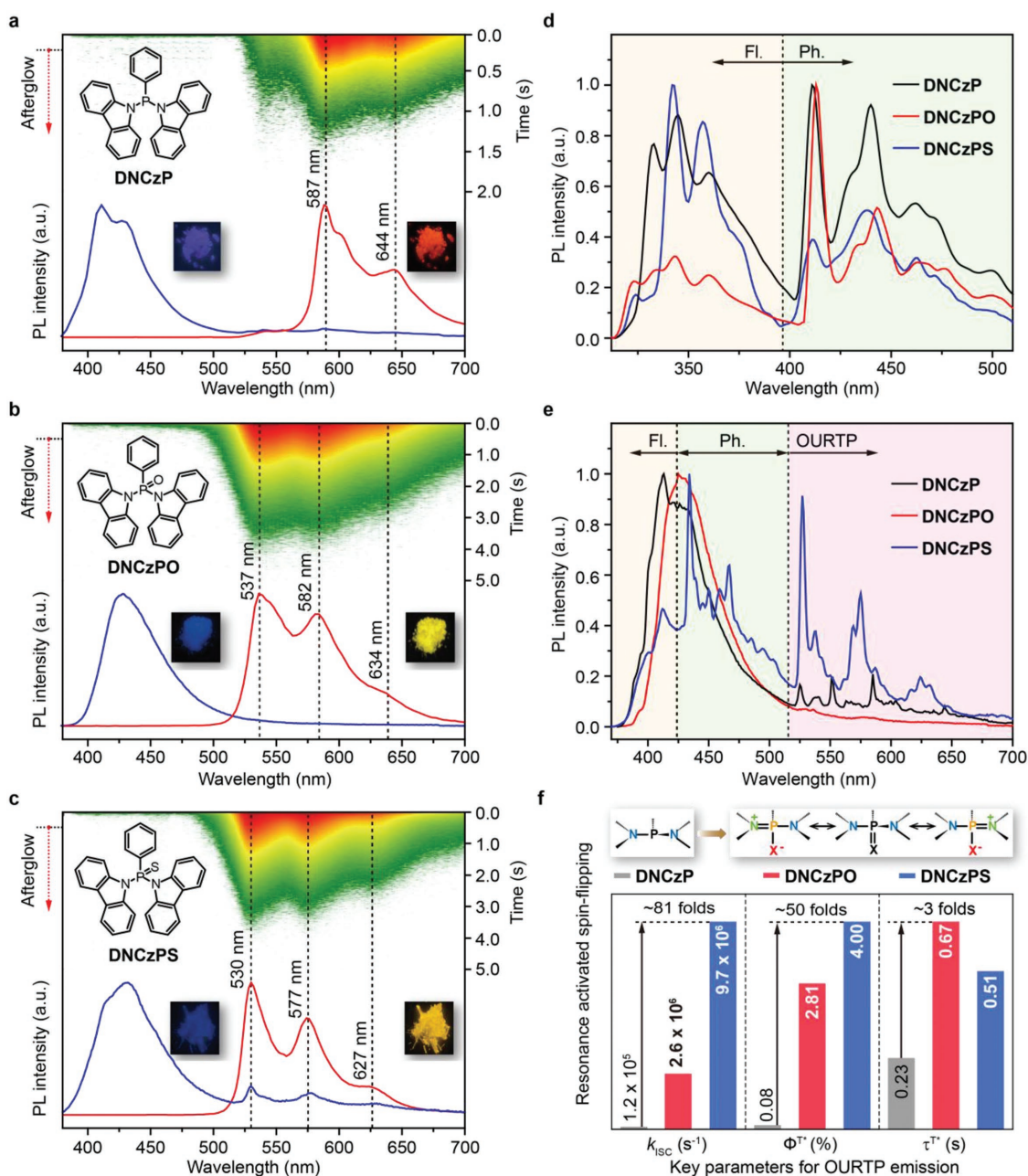


Figure 2. Photophysical properties of the heteroatom-mediated resonance molecules. a–c) Steady-state photoluminescence (blue curve) and time-resolved OURTP (red curve, delay 200 ms) spectra of a) **DNCzP**, b) **DNCzPO**, and c) **DNCzPS** powders at 300 K; insets show the molecular structures, photographs on excitation (left) and removal (right) of the 365 nm lamp, and transient emission decay images (upper), respectively. Steady-state photoluminescent spectra in d) dilute CH₂Cl₂ solutions and e) solid powders at 77 K; excitation wavelength is at 365 nm for powders and 290 nm for solutions, and the fluorescence (Fl.), phosphorescence (Ph.), and OURTP emission regions are in yellow, green, and red, respectively. f) Enhanced ISC by resonance-activated spin-flipping for efficient OURTP with simultaneously improved efficiency (Φ^{T^*}) and elongated lifetime (τ^{T^*}).

investigations, natural bond orbital (NBO) analysis, and SOC calculations (Figure 3). From the TD-DFT-predicted energy levels of the excited states, quite a lot of triplet excited states (T_n) are close to S_1 in energy with small ΔE_{ST} to support efficient ISC (Tables S3–S5, Supporting Information). Further, facile $S_1 \rightarrow T_n$ channels for ISC can be distinguished by their SOC values through Dalton calculations (Figure 3a–c; Table S6, Supporting Information). Notably, the SOC values of these

heteroatom-containing molecules are significantly larger than those of heteroatom-free organic molecules ($\leq 0.1 \text{ cm}^{-1}$).^[33] Based on both small ΔE_{ST} ($< \pm 0.37 \text{ eV}$) and high SOC values ($> 0.3 \text{ cm}^{-1}$),^[34] the number of facile ISC channels (blue channels) found in **DNCzP**, **DNCzPO**, and **DNCzPS** are 7, 6, and 10, respectively. However, this theoretical revealing is contradictory to the experimental results, which suggest significantly enhanced ISC in resonance molecules of **DNCzPO** and

Table 1. Photoluminescence properties and kinetic parameters of OURTP molecules in powder at 300 and 77 K.^{a)}

Parameters		300 K			77 K		
		DNCzP	DNCzPO	DNCzPS	DNCzP	DNCzPO	DNCzPS
Fluorescence	λ [nm]	411, 430	430	414, 430	411, 430	430	414, 430
	τ^F [ns]	6.9, 6.8	10.9	4.2, 5.4	8.6, 8.2	12.8	4.7, 5.8
	Φ^F [%]	4.89	29.90	10.5	7.97	44.86	17.90
	k_r^F [s ⁻¹]	7.1×10^6	2.7×10^7	2.5×10^7	9.3×10^6	3.5×10^7	3.8×10^7
	k_{nr}^F [s ⁻¹]	1.4×10^8	6.2×10^7	2.1×10^8	1.0×10^8	3.9×10^7	8.6×10^7
ISC	ΔE_{ST} [eV]	0.70	0.84	0.81	0.70	0.84	0.81
	k_{ISC} [s ⁻¹]	1.2×10^5	2.6×10^6	9.7×10^6	3.2×10^5	4.5×10^6	8.9×10^7
OURTP	λ [nm]	587, 644	537, 582	530, 577, 627	587, 644	537, 582	530, 577, 627
	τ^{T^*} [s]	0.23, 0.21	0.67, 0.66	0.51, 0.47, 0.43	0.78, 0.69	1.11, 1.12	0.78, 0.76, 0.75
	Φ^{T^*} [%]	0.08	2.81	4.00	0.28	5.74	41.70
	$k_r^{T^*}$ [s ⁻¹]	4.35	1.49	1.96	1.28	0.91	1.28

^{a)}Kinetic parameters of fluorescence and OURTP are obtained according to Equations (S1)–(S10) in the Supporting Information and ΔE_{ST} was measured in dilute CH₂Cl₂ solution.

DNCzPS with much higher k_{ISC} than that of **DNCzP** in both solution and solid state at both room temperature and 77 K (Table 1; Table S2, Supporting Information). Therefore, the resonance variation must play a key role in promoting ISC. First, the energy levels of S_1 and T_n are no longer constant in resonance molecules, but will vary within a certain range of E_{RV} due to the self-adaptive resonance variation, leading to remarkably reduced ΔE_{ST} (real-time ΔE_{ST}) to facilitate ISC based on the energy-gap law (Figure 3d; Figure S18, Supporting Information). Second, the resonance variation with lone-pair electron redistribution will lead to a large change of n-orbital participation ($\Delta\alpha_n$, $\Delta\alpha_n = |\alpha_{n, S1} - \alpha_{n, Tn}|$) for efficient $S_1 \rightarrow T_n$ ISC process with enlarged SOC values,^[3,34] according to the El-Sayed rule (Figure 1b; Figure S19, Supporting Information). Consequently, the low-lying triplet excited states excluded by energy gap law can be activated by resonance variation with E_{RV}^{T1} up to 1.66 eV in **DNCzPO**; also, the low SOC values of the $S_1 \rightarrow T_n$ channels can be significantly enlarged due to large $\Delta\alpha_n$ up to 78% during resonance variation. With the aid of resonance-activated T_n energy (red channels in Figure 3b,c) and resonance enhanced SOC (black channels in Figure 3b), more facile ISC channels are available in the resonance molecules; through this self-adaptive regulation, the experimentally observed significantly enhanced ISC in **DNCzPO** and **DNCzPS** can be well explained and theoretically understood. Although the only structural difference between **DNCzPO** and **DNCzPS** is that O of **DNCzPO** is replaced by S in **DNCzPS**, the larger numbers of available ISC channels with larger SOC values in **DNCzPS** could be mainly due to its relatively small E_{RV} , which renders facile resonance variations to reduce ΔE_{ST} and enhance lone-pair electron redistribution for spin-flipping.

For efficient OURTP emission, the successfully populated T_1 state via resonance-promoted ISC should be further stabilized to slow down both the radiative and nonradiative decay rates for long-lived excited states and emission. H-aggregation is highly effective in trapping the excited states in low-lying aggregation-split energy level for the significantly redshifted OURTP emissions.^[35–37] To identify the existence of the H-aggregation in the

solid state, the single crystal structures of **DNCzP**, **DNCzPO**, and **DNCzPS** were investigated. According to the molecular exciton theory (Equation (1)), the positive exciton splitting energy ($\Delta\epsilon$) of the selected molecular packing manifests the presence of H-aggregates^[38,39]

$$\Delta\epsilon = \frac{2|M|^2}{r_{uv}^3}(\cos\alpha - 3\cos\theta_1\cos\theta_2) \quad (1)$$

where M represents the electric dipole transition moment, r_{uv} is the intermolecular distance between the molecular pair, α is the angle between the transition dipole moments of the two molecules, and θ_1 and θ_2 are angles between transition dipole moments of the two molecules and the interconnection of their molecular centers, respectively. Based on this criterion, various forms of H-aggregation can be figured out. From Figure 3e–h, large and positive $\Delta\epsilon$ values for strong H-aggregation can be observed in resonance molecules of **DNCzPO** and **DNCzPS**, while the $\Delta\epsilon$ values of **DNCzP** are quite small in their single crystal structures (Tables S7 and S8 and Figures S20 and S21, Supporting Information). Moreover, a large number of H-aggregation forms exist in **DNCzPO** crystal, which could be an important reason for its long OURTP lifetime. From the single crystal structures, all of these materials showed strong interactions of C–H...O/S and C–H... π hydrogen bonds and weak intermolecular π ... π interactions of the stacked carbazole moieties, indicating the effective suppress of nonradiative decay of the triplet excitons through molecular rotation and vibration in the solid state (Figure S22, Supporting Information).^[40–42] In addition, the dense molecular packing in the solid state can effectively prevent the penetration of oxygen and water from the surrounding environment to the excited molecules in triplet states to quench their emission. Hence, strong and long-lasting OURTP, which is stable toward oxygen and water under the ambient conditions, can be successfully established in the solid states of the heteroatom-mediated resonance molecules.

With both systematic experimental investigations and theoretical understandings, a possible mechanism for the

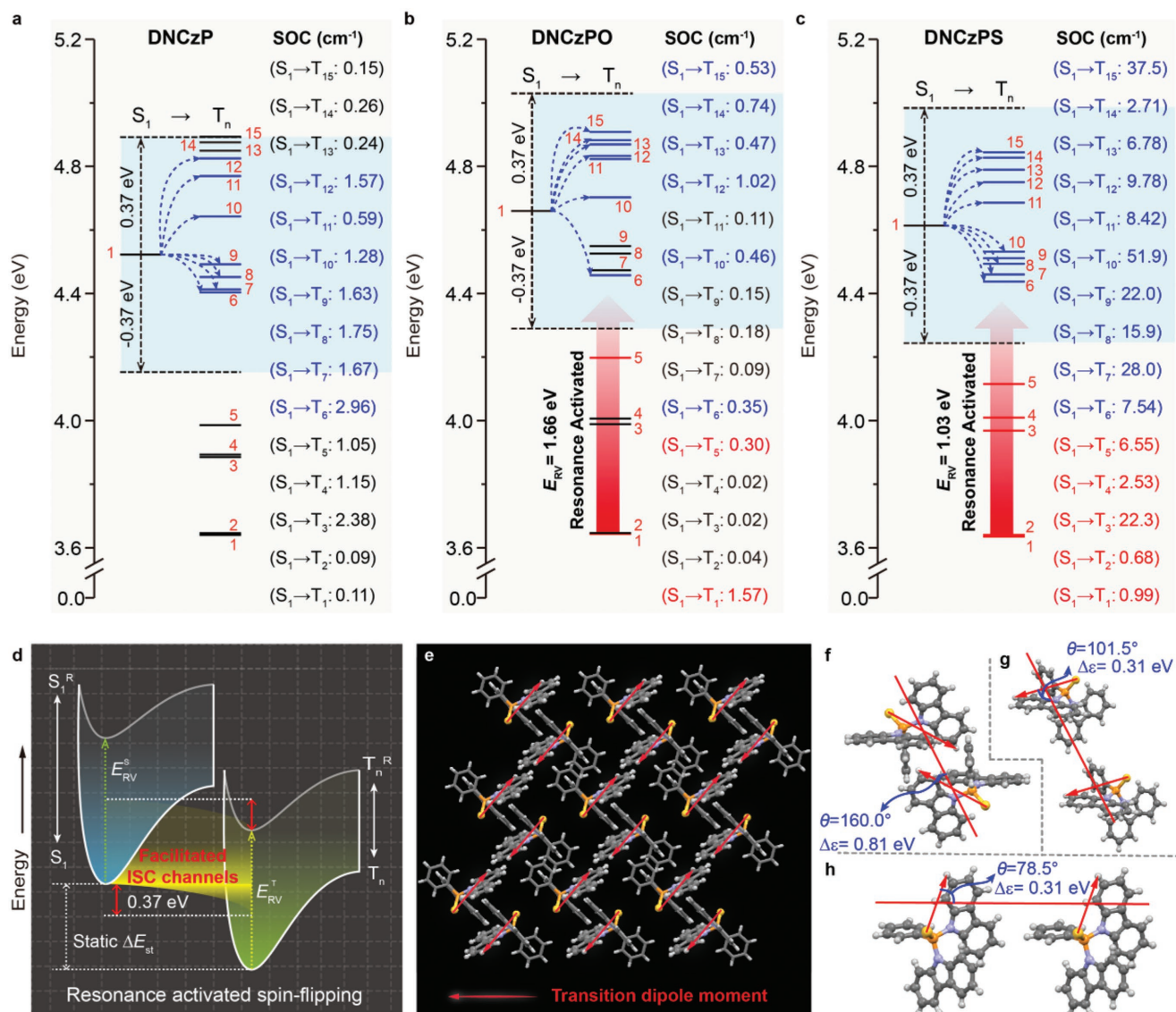


Figure 3. Understanding the resonance-promoted ISC and H-aggregation stabilized triplet exciton for OURTP. a–c) TD-DFT calculated energy level diagram and the corresponding SOC constants of **DNCzP** (a), **DNCzPO** (b), and **DNCzPS** (c). The normal triplet states available for efficient ISC are highlighted in blue, while the resonance-activated triplet states for ISC are in red. d) Schematic drawing of resonance variation facilitated ISC by dynamically reducing ΔE_{ST} (highlight by the yellow color). e) Molecular packing in **DNCzPS** single crystal. f–h) Different H-aggregates evidenced by the positive exciton splitting energy ($\Delta\epsilon$) in **DNCzPS** single crystal.

resonance-promoted OURTP can be proposed: first, the photo-excited singlet excitons is readily transformed to the triplet excitons through facilitated ISC process by reducing ΔE_{ST} and increasing SOC upon resonance variation; second, the effectively populated triplet excitons are subsequently stabilized by the H-aggregation, which further elongate the lifetime of the triplet excited state by reducing both the radiative and nonradiative decay rates and preventing the quenching effects of oxygen and water under the ambient conditions; finally, the stabilized triplet excitons decay radiatively to the ground state in a slow rate for OURTP emission (Figure 4a). Thus, the lifetime of OURTP can reach 0.67 s in **DNCzPO** at room temperature and the ISC rate can be promoted up to $9.7 \times 10^6 \text{ s}^{-1}$ in **DNCzPS** owing to the significantly enhanced resonance variation.

In light of the significantly different ultralong lifetime and color between the fluorescence and OURTP emission of the heteroatom-mediated resonance molecules, the new-concept time-resolved and color-coded multiple informational QR code can be realized using these promising OURTP materials and commercial fluorescent dyes (Figures S23–S25, Supporting Information). The multilayer QR code contains one top red fluorescence QR code (COO@IAM) layer, one middle blue fluorescence background layer, and one bottom OURTP QR code (COO) layer (Figure 4b–d). Under daylight, the multilayer QR code is almost invisible (Figure 4e). On ultraviolet light excitation (365 nm), the top red QR code could be clearly observed and read by a mobile phone showing the information of “COO@IAM”; the bottom QR code layer with blue emission

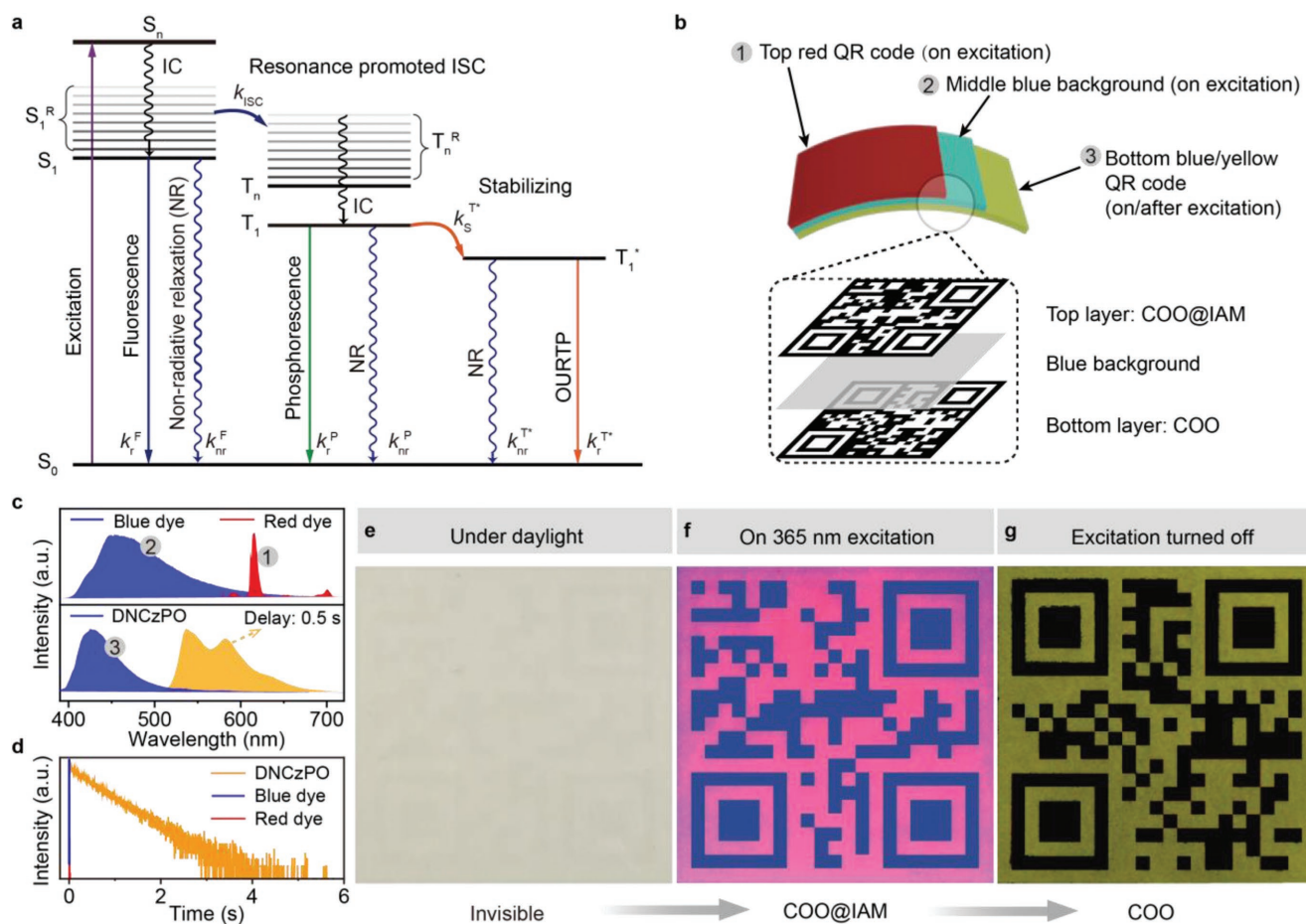


Figure 4. Proposed mechanism for resonance-enhanced OURTP emission and quick response code application. a) Mechanism of the promoted ISC via resonance variation for OURTP emission. b) Construction of time-resolved and color-coded multiple informational QR code using **DNCzPO** powder in combination with red and blue fluorescence dyes in three layers. c) Fluorescent spectra of the red and blue dyes (top) and the steady-state (blue) and OURTP emission spectra (yellow) of **DNCzPO** (bottom) at room temperature. d) Lifetime decay profiles of the short-lived luminescence of the red and blue dyes and the long-lived OURTP emission of **DNCzPO**. e–g) Multiple informational QR code under daylight (e), on 365 nm excitation (f), and after removal of the excitation (g).

under UV light excitation is virtually invisible because of the background fluorescence interference of the middle blue layer (Figure 4f). After the switching off of the UV light, the short-lived red and blue fluorescence disappears immediately; the bottom QR code with yellow OURTP emission appears and can be read easily by the mobile phone to get the secondary or encrypted information of “COO” (Figure 4g; Movie S1, Supporting Information).

In summary, we demonstrate a dynamic approach to promote spin-flipping of purely organic molecules for high ISC and high-performance OURTP emission by using heteroatom-mediated resonance variation for the first time. Contrast to current static-state techniques in manipulating ISC with small ΔE_{ST} , our strategy via resonance structure can remarkably boost ISC at large ΔE_{ST} through dynamically varied excited energies of resonance canonical forms and a large change of n-orbital participation by redistribution of lone-pair electrons upon resonance variation. Consequently, the resonance molecules of **DNCzPO** and **DNCzPS** exhibited significantly facilitated spin-flipping with ISC rate constant up to $9.7 \times 10^6 \text{ s}^{-1}$ and OURTP

emission with a long lifetime of $\approx 0.67 \text{ s}$ and a high quantum efficiency of 4.0% at room temperature, which are 81-, 3-, and 50-folds higher than that of **DNCzP**. With the distinguished ultralong lifetime, high efficiency, and color variation of the OURTP emission, the time-resolved and color-coded QR code capable of showing different encrypted information was successfully fabricated and readily readable by commercial mobile phones. The concept of resonance modulation of energy-gap law and the intrinsic competition between the OURTP lifetime and efficiency, would be highly attractive for the development of purely organic phosphorescent materials, presenting a major step forward in understanding the excited state manipulation of organic molecules and could initiate dynamic attempts to boost ISC for new-concept materials and devices.

Supporting Information

Supporting Information is available from the Wiley Online Library or from the author.

Acknowledgements

This study was supported in part by the National Natural Science Foundation of China (Grant Nos. 21674049, 21772095, 21604039, 21704042, and 21703077), Science Fund for Distinguished Young Scholars of Jiangsu Province of China (Grant No. BK20150041), 1311 Talents Program of Nanjing University of Posts and Telecommunications (Dingshan), the Six Talent Plan of Jiangsu Province (Grant No. 2016XCL050), National Postdoctoral Program for Innovative Talents (BX201600071) and China Postdoctoral Science Foundation funded project (Grant No. 2016M600403), Jiangsu Planned Projects for Postdoctoral Research Funds (Grant No. 1701036A) and the Natural Science Fund for Colleges and Universities in Jiangsu Province (Grant No. 17KJB150017), Science and Technology Development Program of Henan province (Grant No. 172102310164).

Conflict of Interest

The authors declare no conflict of interest.

Keywords

dynamic activation, organic afterglow, organic ultralong room-temperature phosphorescence, resonance molecules, spin-flipping

Received: June 18, 2018

Revised: August 3, 2018

Published online: September 10, 2018

- [1] R. Kabe, C. Adachi, *Nature* **2017**, *550*, 384.
- [2] Z. An, C. Zheng, Y. Tao, R. Chen, H. Shi, T. Chen, Z. Wang, H. Li, R. Deng, X. Liu, W. Huang, *Nat. Mater.* **2015**, *14*, 685.
- [3] Z. He, W. Zhao, J. W. Y. Lam, Q. Peng, H. Ma, G. Liang, Z. Shuai, B. Z. Tang, *Nat. Commun.* **2017**, *8*, 416.
- [4] Q. Miao, C. Xie, X. Zhen, Y. Lyu, H. Duan, X. Liu, J. V. Jokerst, K. Pu, *Nat. Biotechnol.* **2017**, *35*, 1102.
- [5] S. Hirata, *Adv. Opt. Mater.* **2017**, *5*, 1700116.
- [6] Y. Shoji, Y. Iwabata, Q. Wang, D. Nemoto, A. Sakamoto, N. Tanaka, J. Seino, H. Nakai, T. Fukushima, *J. Am. Chem. Soc.* **2017**, *139*, 2728.
- [7] J. Yang, X. Zhen, B. Wang, X. Gao, Z. Ren, J. Wang, Y. Xie, J. Li, Q. Peng, K. Pu, Z. Li, *Nat. Commun.* **2018**, *9*, 840.
- [8] R. Gao, X. Mei, D. Yan, R. Liang, M. Wei, *Nat. Commun.* **2018**, *9*, 2798.
- [9] R. Gao, D. Yan, *Chem. Sci.* **2017**, *8*, 590.
- [10] R. Kabe, N. Notsuka, K. Yoshida, C. Adachi, *Adv. Mater.* **2016**, *28*, 655.
- [11] S. Cai, H. Shi, J. Li, L. Gu, Y. Ni, Z. Cheng, S. Wang, W. Xiong, L. Li, Z. An, W. Huang, *Adv. Mater.* **2017**, *29*, 1701244.
- [12] Z. Yang, Z. Mao, X. Zhang, D. Ou, Y. Mu, Y. Zhang, C. Zhao, S. Liu, Z. Chi, J. Xu, Y. Wu, P. Lu, A. Lien, M. R. Bryce, *Angew. Chem., Int. Ed.* **2016**, *55*, 2181.
- [13] C. Li, X. Tang, L. Zhang, C. Li, Z. Liu, Z. Bo, Y. Q. Dong, Y. Tian, Y. Dong, B. Z. Tang, *Adv. Opt. Mater.* **2015**, *3*, 1184.
- [14] Z. Cheng, H. Shi, H. Ma, L. Bian, Q. Wu, L. Gu, S. Cai, X. Wang, W. Xiong, Z. An, W. Huang, *Angew. Chem., Int. Ed.* **2018**, *57*, 678.
- [15] X. Zhen, Y. Tao, Z. An, P. Chen, C. Xu, R. Chen, W. Huang, K. Pu, *Adv. Mater.* **2017**, *29*, 1606665.
- [16] S. M. A. Fateminia, Z. Mao, S. Xu, Z. Yang, Z. Chi, B. Liu, *Angew. Chem., Int. Ed.* **2017**, *56*, 12160.
- [17] Z. Yang, Z. Mao, Z. Xie, Y. Zhang, S. Liu, J. Zhao, J. Xu, Z. Chi, M. P. Aldred, *Chem. Soc. Rev.* **2017**, *46*, 915.
- [18] Y. Tao, K. Yuan, T. Chen, P. Xu, H. Li, R. Chen, C. Zheng, L. Zhang, W. Huang, *Adv. Mater.* **2014**, *26*, 7931.
- [19] J. Xia, S. N. Sanders, W. Cheng, J. Z. Low, J. Liu, L. M. Campos, T. Sun, *Adv. Mater.* **2017**, *29*, 1601652.
- [20] T. N. Singh-Rachford, F. N. Castellano, *Coord. Chem. Rev.* **2010**, *254*, 2560.
- [21] G. Baryshnikov, B. Minaev, H. Ågren, *Chem. Rev.* **2017**, *117*, 6500.
- [22] S. Xu, R. Chen, C. Zheng, W. Huang, *Adv. Mater.* **2016**, *28*, 9920.
- [23] H. Uoyama, K. Goushi, K. Shizu, H. Nomura, C. Adachi, *Nature* **2012**, *492*, 234.
- [24] S. K. Lower, M. A. El-Sayed, *Chem. Rev.* **1966**, *66*, 199.
- [25] W. Zhao, Z. He, J. W. Y. Lam, Q. Peng, H. Ma, Z. Shuai, G. Bai, J. Hao, B. Z. Tang, *Chem* **2016**, *1*, 592.
- [26] Y. Tao, J. Xiao, C. Zheng, Z. Zhang, M. Yan, R. Chen, X. Zhou, H. Li, Z. An, Z. Wang, H. Xu, W. Huang, *Angew. Chem., Int. Ed.* **2013**, *52*, 10491.
- [27] Y. Tao, L. Xu, Z. Zhang, R. Chen, H. Li, H. Xu, C. Zheng, W. Huang, *J. Am. Chem. Soc.* **2016**, *138*, 9655.
- [28] H. Yang, Q. Liang, C. Han, J. Zhang, H. Xu, *Adv. Mater.* **2017**, *29*, 1700553.
- [29] M. Y. Berezin, S. Achilefu, *Chem. Rev.* **2010**, *110*, 2641.
- [30] X. Yang, D. Yan, *Adv. Opt. Mater.* **2016**, *4*, 897.
- [31] X. Yang, X. Lin, Y. Zhao, Y. S. Zhao, D. Yan, *Angew. Chem., Int. Ed.* **2017**, *56*, 7853.
- [32] J. Yang, Z. Ren, Z. Xie, Y. Liu, C. Wang, Y. Xie, Q. Peng, B. Xu, W. Tian, F. Zhang, Z. Chi, Q. Li, Z. Li, *Angew. Chem., Int. Ed.* **2017**, *56*, 880.
- [33] Y. Gong, L. Zhao, Q. Peng, D. Fan, W. Z. Yuan, Y. Zhang, B. Z. Tang, *Chem. Sci.* **2015**, *6*, 4438.
- [34] R. Chen, Y. Tang, Y. Wan, T. Chen, C. Zheng, Y. Qi, Y. Cheng, W. Huang, *Sci. Rep.* **2017**, *7*, 6225.
- [35] D. Chaudhuri, D. Li, Y. Che, E. Shafran, J. M. Gerton, L. Zang, J. M. Lupton, *Nano Lett.* **2011**, *11*, 488.
- [36] F. Meinardi, M. Cerminara, A. Sassella, R. Bonifacio, R. Tubino, *Phys. Rev. Lett.* **2003**, *91*, 247401.
- [37] E. Lucenti, A. Forni, C. Botta, L. Carlucci, C. Giannini, D. Marinotto, A. Previtali, S. Righetto, E. Cariati, *J. Phys. Chem. Lett.* **2017**, *8*, 1894.
- [38] M. Kasha, H. R. Rawls, M. Ashraf El-Bayoumi, *Pure Appl. Chem.* **1965**, *11*, 371.
- [39] E. G. McRae, M. Kasha, *Physical Processes in Radiation Biology*, Academic Press, New York **1964**.
- [40] W. Z. Yuan, X. Y. Shen, H. Zhao, J. W. Y. Lam, L. Tang, P. Lu, C. Wang, Y. Liu, Z. Wang, Q. Zheng, J. Z. Sun, Y. Ma, B. Z. Tang, *J. Phys. Chem. C* **2010**, *114*, 6090.
- [41] Y. Xie, Y. Ge, Q. Peng, C. Li, Q. Li, Z. Li, *Adv. Mater.* **2017**, *29*, 1606829.
- [42] O. Bolton, K. Lee, H. Kim, K. Y. Lin, J. Kim, *Nat. Chem.* **2011**, *3*, 205.